Available online at www.sciencedirect.com

ScienceDirect

Energy Procedia 55 (2014) 539 – 544

Energy Procedia

4th International Conference on Silicon Photovoltaics, SiliconPV 2014

Internal gettering of iron at extended defects

Michael Knörlein[a], Antoine Autruffe[a], Rune Søndenå[b], Marisa Di Sabatino[a,]*

[a]*Norwegian University of Science and Technology, Dep Materials Science and Engineering, Trondheim 7491, Norway*
[b]*Institute for Energy Technology, Dep of Solar Energy, Kjeller 2007, Norway*

Abstract

The role of iron in crystalline silicon solar cells has been extensively investigated, yet the interaction mechanisms with structural defects have not been fully understood. In this work we have investigated a multicrystalline silicon ingot made in a small scale (1.5 kg) vertical gradient freeze (VGF) furnace with the addition of 50 ppma Fe in the polysilicon feedstock. The minority carrier lifetime was qualitatively measured by photoluminescence (PL). Grain morphology and -orientation were determined by electron backscatter diffraction (EBSD). The comparison between the PL and EBSD maps shows high lifetime areas near the grain boundaries, which is explained by an internal gettering mechanism. Furthermore, it is evident that Fe segregates slightly at coincidence site lattice (CSL) boundaries – especially at Σ3, while it segregates heavily at random grain boundaries. These results indicate the dependence of Fe segregation towards defect on grain boundary character. A method to qualitatively and quantitatively identify the segregation profiles and depleted region thickness is developed by image analysis.

© 2014 The Authors. Published by Elsevier Ltd. This is an open access article under the CC BY-NC-ND license (http://creativecommons.org/licenses/by-nc-nd/3.0/).
Peer-review under responsibility of the scientific committee of the SiliconPV 2014 conference

Keywords: silicon; iron; gettering; defects.

1. Introduction

Multicrystalline silicon (mc-Si) represents 50% of the total PV production and is a cheaper alternative to monocrystalline materials. However, relative higher concentrations of impurities and structural defects limit the efficiency of mc-Si solar cells [1, 2]. The role of crystallization processes for defect and impurity distribution has been recently reviewed [3]. During ingot solidification and subsequent cooling, impurities segregate towards grain

* Corresponding author. Tel.: +47-735-51-205; fax: +47-735-50-203.
E-mail address: Marisa.di.sabatino@material.ntnu.no

1876-6102 © 2014 The Authors. Published by Elsevier Ltd. This is an open access article under the CC BY-NC-ND license (http://creativecommons.org/licenses/by-nc-nd/3.0/).
Peer-review under responsibility of the scientific committee of the SiliconPV 2014 conference
doi:10.1016/j.egypro.2014.08.021

boundaries and dislocation clusters. This phenomenon, known as internal gettering (IG), results in an increase of defects recombination activities [4, 5] and the appearance of regions of low impurity concentration [6, 7], i.e. depleted regions. IG of metallic impurities has also been identified as a limitation to the efficiency of external gettering (EG) [8, 9].

Iron is an impurity which is always present in multicrystalline silicon ingots due to in-diffusion from, primarily, the crucible and coating materials. The effect of iron in mc-Si solar cells has been previously investigated [10]. Still internal gettering of iron and its interaction with extended defects, e.g. grain boundaries and dislocations, remain to be fully understood. In this work iron gettering behavior is investigated using qualitative minority carrier lifetime imaging method. Despite its simplicity the method is a useful tool to qualitatively and quantitatively compare the role of different types of grain boundaries (GBs). Internal gettering towards GBs is assessed and grain boundary nature influence on segregation profile and intensity is discussed.

2. Experimental

A multicrystalline silicon ingot of approximately 1.5 kg was solidified in a vertical gradient freeze (VGF) furnace that was built in our laboratory. The furnace has two (top and bottom) resistance heaters. It was doped with boron to achieve a target resistivity of 1 Ωcm and 50 ppma Fe was added to the polysilicon feedstock. At the beginning of solidification, the temperature difference between top and bottom heaters was approximately 550 K. Selected samples, cut perpendicularly to the growth direction, were polished, etched and passivated. Qualitative minority carrier lifetime maps were obtained by photoluminescence (PL) imaging. Grain orientation and grain boundary characters were determined by electron backscatter diffraction (EBSD) using scanning electron microscope (SEM).

A sample taken at approximately 85% ingot height was selected for studying the effect of grain boundary nature on Fe distribution. The method developed consists of calculation of the highest contrast value of the fitted Gaussian curves. The method also allows calculating the thickness of the area around the grain boundary where iron concentration suddenly decreases, the so-called *depleted region*. The data are taken from the PL images of silicon wafers. The full width of tenth maximum (FWTM) for a Gaussian curve is:

$$\Delta d = 2\sqrt{2\ln 10 c} \quad (1)$$

Nomenclature

Δd width of the depleted regions
c two inflection points of the function occur at $x=b-c$ and $x=b+c$

Phosphorus gettering [11, 12] was performed on a neighboring sample, taken at approximately 85% ingot height, by in-diffusion of a phosphorus emitter (50 Ω/sq.) in a $POCl_3$ tube furnace followed by an emitter etch-back. The sample was surface passivated using hydrogenated amorphous silicon. The interstitial iron concentration in the ungettered sample was measured by FeB pair dissociation using micro-wave photoconductance decay (µw-PCD) [13, 14]. Photoluminescence imaging was performed using a LIS-R1 setup from BTI [15, 16]. A diode laser with a wavelength of 808 nm is used to illuminate the sample and the resulting band-to-band photoluminescence is measured with a CCD camera. A lifetime map is obtained by quasi-steady state photoconductance (QSSPC) and used for the calibration of the PL-signal.

3. Results and discussion

Figure 1a shows the PL image of an unpassivated horizontal sample taken from about 53% of the ingot height illuminated for 30 seconds using an 808 nm laser. Assuming uniform surface properties, both optical and electrical, the PL signal scales with the minority carrier lifetime in the sample. Thus, qualitative evaluation of the electrical properties of the samples is enabled. Higher PL-signal in grain boundaries and dislocation clusters are usually

observed in wafers containing large amounts of metallic impurities, e.g. in the red zones of multicrystalline ingots [17]. Areas where the iron concentration is low coincide with the high PL signals, interpreted as high lifetime areas. Most of the grain boundaries are bright in the PL images, indicating high lifetime (hence low electrical recombination) and can be related to low iron concentration. This indicates that there are areas around the grain boundary where iron concentration suddenly decreases. This is attributed to internal gettering of Fe at the grain boundary (GB) resulting in a Fe depleted region with a corresponding high lifetime close to the GB [18]. A schematic view of this mechanism is given in Figure 1b. Iron accumulates at the GB which is surrounded by low-concentration areas (*depleted regions*). However, PL images allows to revealing only the depleted region, as its resolution is not high enough to show the low lifetime at the GB interface.

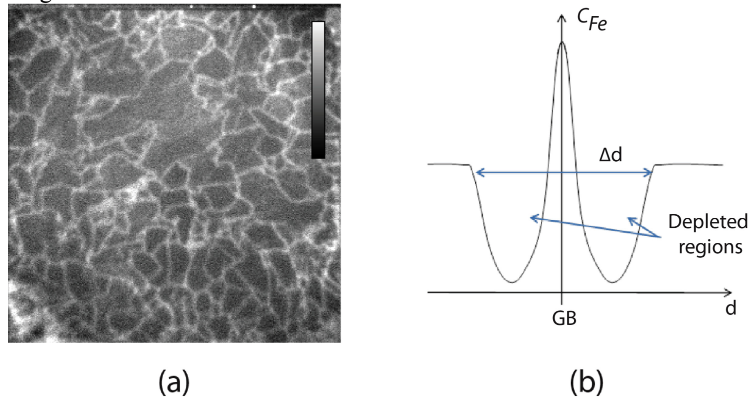

Fig. 1. (a) Uncalibrated PL image of a horizontal cross section taken at 53% height in the ingot. The map shows qualitative high and low lifetime areas. (b) Schematic view of Fe concentration (C_{Fe}) distribution at grain boundary (GB). On both sides of the GB there are areas of low Fe concentration (depleted regions).

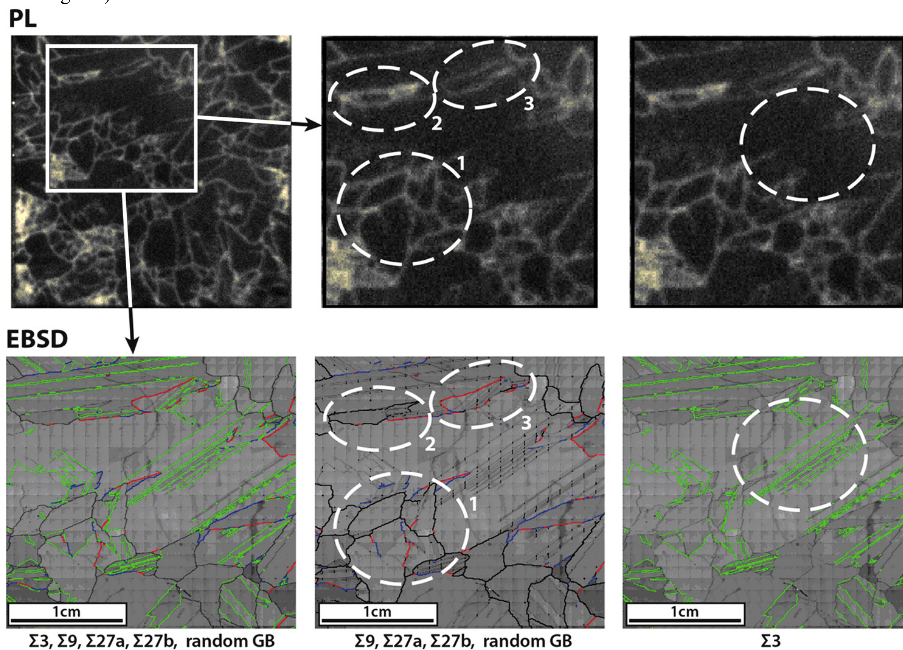

Fig. 2. Comparison between EBSD maps (bottom) and a PL map (top) from a horizontal cross section sample taken at approximately 85% fraction solid. On the EBSD maps, grain boundary characters are indicated by color – i.e. Σ3 in green, Σ9 in blue, Σ27 in red and random GB in black.

Figure 2 shows a comparison between the EBSD micrographs and PL images. It is observed that different types of grain boundary have different PL contrast. As previously observed [4], very limited or no Fe segregation towards Σ3 is detected, and a slight segregation is observed at Σ9 grain boundaries. In Σ27 and random grain boundaries the internal gettering effect is more pronounced, as they show higher contrast on PL maps. It has been reported that the initial iron level has a major impact on gettering efficiency and that for levels below 1×10^{12} cm^{-3} (i.e. <0.02 ppba) IG is practically impossible to achieve by cooling [19]. The Fe pollution level in the ingot investigated is 50 ppma. Because the Fe equilibrium partition ratio reported in literature is ~ $8x10^{-6}$ [19], the initial content in the solid can be expected to be ~0.4 ppba (thus higher than 0.02 ppba).

Grain boundary segregation profiles are assessed as a function of their nature. Image analyses methods are used to compare the depleted region thicknesses and the segregation intensity. Contrast values are extracted from a PL image, around a selected grain boundary. The resulting data are fitted to a Gauss curve, giving the maximum contrast value at the grain boundary and, the width of the bright band, i.e. the depleted region, at the grain boundary. This width is evaluated by calculating the full width at tenth of the Gauss curve maximum (FWTM) and by using Equation (1). Grain boundary nature influence on both maximum contrast and depleted region width is assessed. Figure 3 shows the contract index results for all types of grain boundaries investigated, namely Σ3, Σ9, Σ27, and random GB, respectively. These results indicate that Σ3 GBs have no visible gettering effect whereas the effect of Σ9 and Σ27 GBs is more pronounced. These results are in agreement with the calculations made by Kohyama et al. [20]. The authors showed that the interfacial energy of a <110> tilt GB depends on its character and misorientation angle. Σ3 interfacial energy was found to be close to 0 Jm^{-2} while Σ9 and Σ27 interfacial energies are significantly higher. Random GBs show the highest contrast indicating the strongest internal gettering effect. Furthermore, the thickness of the depleted regions is approximately the same and only the contrast (i.e. the internal gettering efficiency) changes for the different GBs. This indicates that the extension of the depleted region is mainly dominated by the diffusion length of iron.

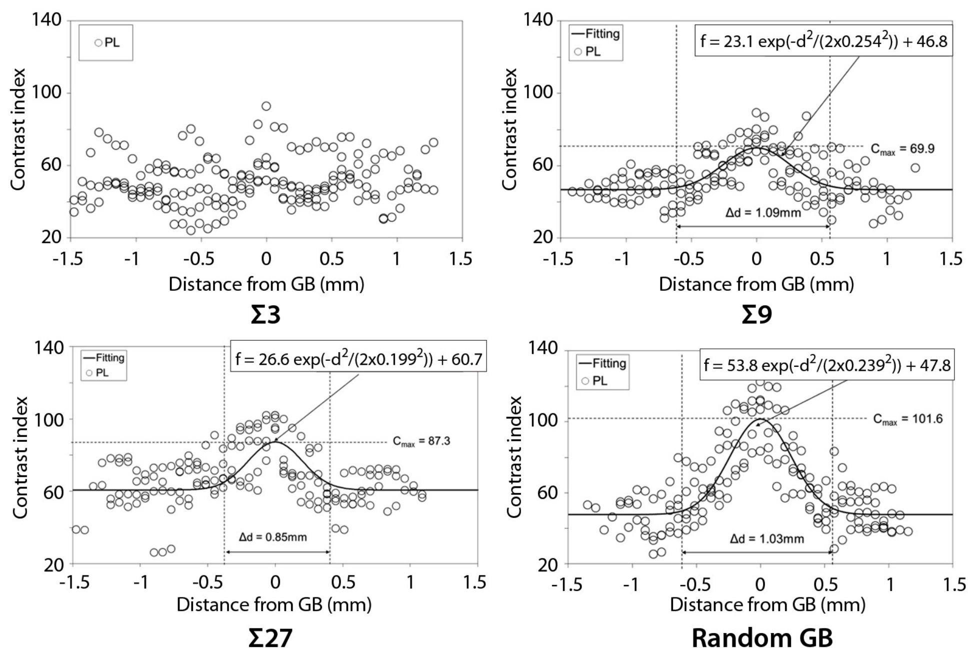

Fig. 3. Contrast indices as extracted from PL maps, for different grain boundary characters; Σ3, Σ9, Σ27, and random GB, respectively. The indices are fitted to Gauss curves. Maximum contrast C_{max}, and depleted region thickness Δd are evaluated for each GB.

Figure 4 presents the PL map of the selected mc-Si sample before and after gettering. If comparable surface properties are assumed in Figures 4a and 4b, the increase in the PL-signal following the P gettering process leads to

an increase in lifetime. The P gettering increases the PL-signal by roughly a factor of 6, both in large grains as well as across the grain boundaries. Only in the dislocation clusters, represented as large bright areas, the effect of P gettering is reduced. An example of limited impact of EG in a dislocated region is highlighted with a red circle on Fig.4. It is well known that the beneficial effect of gettering is limited in areas with high dislocation densities [13, 21]. The minority carrier lifetime in a passivated wafer after gettering is shown in Figure 4c. A mean lifetime across the wafer of 25 µs (max. 62 µs) is obtained, from the QSSPC calibrated PL image.

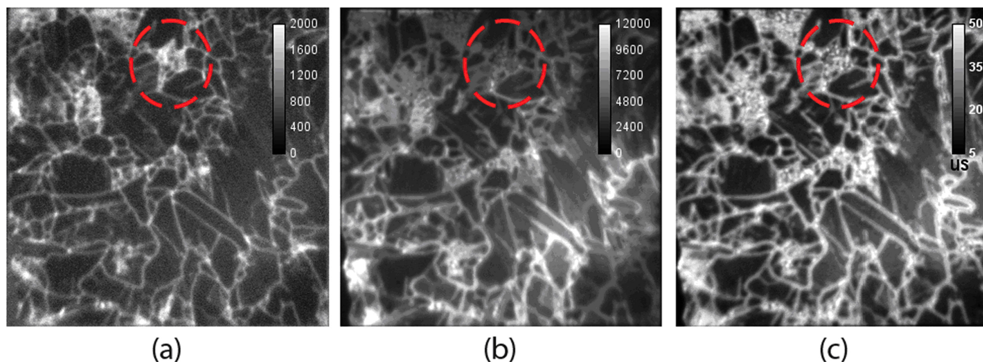

Fig. 4. Uncalibrated PL images (30 s illumination) before (a) and after P gettering (b) shows that lifetime improves about six times. The minority carrier lifetime on a surface passivated wafer using QSSPC calibrated PL imaging is shown in (c).

4. Conclusions

A multicrystalline silicon ingot intentionally contaminated with iron was produced in a small scale VGF furnace. The behavior of iron in the material was studied by PL and EBSD. A quantitative method to compare the effects of different GBs was developed. The method uses PL data to calculate contrast values of the fitted Gaussian curves. During solidification iron close to the grain boundaries diffuses to these GBs, leaving behind depleted regions with lower iron concentrations and, therefore, higher minority carrier lifetimes. The contrast values based on the PL images together with the EBSD maps show that the different grain boundaries have different effect on the near-lying iron. Σ3 GBs show no visible internal gettering effect whereas the effect of Σ9 and Σ27 GBs is more pronounced. Random GBs show the highest contrast indicating the strongest internal gettering effect. The results show that the width of the depleted regions is approximately the same and only the contrast (i.e. the gettering efficiency) changes for the different GBs.

Acknowledgements

This work has been performed within the Norwegian research Centre for Solar Cell Technology, co-sponsored by the Norwegian Research Council and industry partners.

References

[1] C. Donolato, Modeling the effect of dislocations on the minority carrier diffusion length of a semiconductor, J. Appl. Phys. 84 (1998) 2656-2664.
[2] G. Coletti, Sensitivity of state-of-the-art and high efficiency crystalline silicon solar cells to metal impurities, Prog. Photovolt.: Res. Appl. 21 (2013) 1163-1170.
[3] M. Di Sabatino and G. Stokkan, Defect generation, advanced crystallization and characterization methods for high-quality solar-cell silicon, Phys. Status Solidi 210 (2013) 641-648.

[4] J. Chen, T. Sekiguchi, D. Yang, F. Yin, K. Kido, S. Tsurekawa, Electron-beam-induced current study of grain boundaries in multicrystalline silicon, J. Appl. Phys. 96 (2004) 5490-5495.
[5] M.I. Bertoni, D.P. Fenning, M. Rinio, V. Rose, M. Holt, J. Maser, T. Buonassisi, Nanoprobe X-ray fluorescence characterization of defects in large-area solar cells, Energy & Enviromental Science 4 (2011) 4252-4257.
[6] A. Autruffe, L. Vines, L. Arnberg, M. Di Sabatino, Impact of growth rate on impurities segregation at grain boundaries in silicon during Bridgman growth, J. Cryst. Growth 372 (2013) 180-188.
[7] S. Martinuzzi, I. Périchaud, O. Palais, Segregation phenomena in large-size cast multicrystalline Si ingots, Sol. En. Mat. Sol. Cells 91 (2007) 1172-1175.
[8] I. Périchaud, Gettering of impurities in solar silicon, Sol. En. Mat. Sol. Cells 72 (2002) 315-326.
[9] S.A. Mchugo, Release of metal impurities from structural defects in polycrystalline silicon, Appl. Phys. Lett. 71 (1997) 1984-1986.
[10] G. Coletti, R. Kvande, V.D. Mihailetchi, L.J. Geerligs, L. Arnberg, E.J. Øvrelid, effect of iron in silicon feedstock on p- and n-type multicrystalline silicon, J. Appl. Phys. 104 (2008) 104913.
[11] A. Bentzen, A. Holt, R. Kopecek, G. Stokkan, J.S. Christensen, B.G. Svensson, Gettering of transition metal impurities during phosphorus emitter diffusion in multicrystalline silicon solar cell processing, J. Appl. Phys. 99 (2006) 093509.
[12] A. Bentzen, A. Holt, Overview of phosphorus diffusion and gettering in multicrystalline silicon, Mat. Sci. Eng. B, 159-160 (2009) 228.
[13] D. Macdonald, J. Tan, T. Trupke, Imaging interstitial iron concentrations in boron-doped crystalline silicon using photoluminescence, J. Appl. Phys. 103 (2008) 073710.
[14] D. Macdonald, T. Roth, P.N.K. Deenapanray, T. Trupke, R.A. Bardos, Doping dependence of the carrier lifetime crossover point upon dissociation of iron-boron pairs in crystalline silicon, Appl. Phys. Lett. 89 (2006) 142107.
[15] T. Trupke, R.A. Bardos, M.C. Schubert, W. Warta, Photoluminescence imaging of silicon wafers, Appl. Phys. Lett. 89 (2006) 044107.
[16] T. Trupke, B. Mitchell, J.W. Weber, W. McMillan, R.A. Bardos, R. Kroeze, Photoluminescence imaging for photovoltaic applications, Energy Procedia 15 (2012) 135-146.
[17] Y. Boulfrad, A. Haarahiltunen, H. Savin, E.J. Øvrelid, L. Arnberg, Enhanced performace in the deteriorated area of mc-Si wafers by internal gettering, IEEE J. Photovolt. 2 (2012) 479-484.
[18] A. Haarahiltunen, Heterogeneous precipitation and internal gettering efficiency of iron in silicon, PhD Thesis at Aalto University, 2007.
[19] R. Hull, Properties of Crystalline Silicon, No. 20, Institution of Engineering and Technology, 1999.
[20] M. Kohyama, R. Yamamoto, M. Doyama, Reconstructed structures of symmetrical (011) tilt grain-boundaries in silicon, Phys. Status Solidi B 138 (1986) 387-397.
[21] A.A. Istratov, T. Buonassisi, R.J. McDonald, A.R. Smith, R. Schindler, J.A. Rand, J.P. Kalejs, E.R. Weber, Metal content of multicrystalline silicon for solar cells and its impact on minority carrier diffusion length, J. Appl. Phys. 94 (2003) 6552-6559.